DOI:10.1093/jnci/djt153
Advance Access publication July 2, 2013

ARTICLE

Metabolic Alterations in Mammary Cancer Prevention by Withaferin A in a Clinically Relevant Mouse Model

Eun-Ryeong Hahm, Joomin Lee, Su-Hyeong Kim, Anuradha Sehrawat, Julie A. Arlotti, Sruti S. Shiva, Rohit Bhargava, Shivendra V. Singh

Manuscript received October 18, 2012; revised January 22, 2013; accepted May 21, 2013.

Correspondence to: Shivendra V. Singh, PhD, University of Pittsburgh Cancer Institute, 2.32A Hillman Cancer Center Research Pavilion, 5117 Centre Ave, Pittsburgh, PA 15213 (e-mail: singhs@upmc.edu).

Background Efficacy of withaferin A (WA), an Ayurvedic medicine constituent, for prevention of mammary cancer and its associated mechanisms were investigated using mouse mammary tumor virus–*neu* (MMTV-*neu*) transgenic model.

Methods Incidence and burden of mammary cancer and pulmonary metastasis were scored in female MMTV-*neu* mice after 28 weeks of intraperitoneal administration with 100 μg WA (three times/week) (n = 32) or vehicle (n = 29). Mechanisms underlying mammary cancer prevention by WA were investigated by determination of tumor cell proliferation, apoptosis, metabolomics, and proteomics using plasma and/or tumor tissues. Spectrophotometric assays were performed to determine activities of complex III and complex IV. All statistical tests were two-sided.

Results WA administration resulted in a statistically significant decrease in macroscopic mammary tumor size, microscopic mammary tumor area, and the incidence of pulmonary metastasis. For example, the mean area of invasive cancer was lower by 95.14% in the WA treatment group compared with the control group (mean = 3.10 vs 63.77 mm^2, respectively; difference = –60.67 mm^2; 95% confidence interval = –122.50 to 1.13 mm^2; P = .0536). Mammary cancer prevention by WA treatment was associated with increased apoptosis, inhibition of complex III activity, and reduced levels of glycolysis intermediates. Proteomics confirmed downregulation of many glycolysis-related proteins in the tumor of WA-treated mice compared with control, including M2-type pyruvate kinase, phosphoglycerate kinase, and fructose-bisphosphate aldolase A isoform 2.

Conclusions This study reveals suppression of glycolysis in WA-mediated mammary cancer prevention in a clinically relevant mouse model.

J Natl Cancer Inst;2013;105:1111–1122

Breast cancer is a global health concern accounting for nearly 40 000 deaths each year in the United States alone (1). Novel strategies for prevention of breast cancer are needed to reduce morbidity and mortality associated with this disease. Primary prevention of breast cancer is feasible as exemplified by successful clinical application of selective estrogen receptor modulators (eg, tamoxifen and raloxifene) and aromatase inhibitors (eg, exemestane) (2–4). Unfortunately, women with estrogen receptor–negative breast cancer and a subset of women with estrogen receptor–positive breast cancer are not responsive to these endocrine modalities, which also have side effects (2,3,5,6). For example, combined analysis of multiple randomized and controlled trials comparing aromatase inhibitors with tamoxifen revealed higher incidence of grade 3 and 4 cardiovascular events resulting from aromatase inhibitor use (5,6).

Recent literature highlights the merit of plants used in Ayurvedic medicine, which has been practiced for centuries in India for the treatment of different disorders, for identification of novel cancer preventive agents (7). *Withania somnifera* (also known as ashwagandha) is one such medicinal plant with a variety of known pharmacological effects in experimental models, including anticancer effects (8–14). For example, injections of the leaf extract of *W somnifera* every third day to the tumor site resulted in growth retardation of human fibrosarcoma subcutaneously implanted in athymic mice without any adverse side effects (14).

The anticancer effect of *W somnifera* is ascribed to withanolides such as withaferin A (WA) (Figure 1A) (15–21). For example, WA administration for 14 weeks conferred substantial protection against 7,12-dimethylbenz[*a*]anthracene–induced oral cancer in hamsters (17). WA was shown to inhibit growth of human cancer cells in culture and in vivo in association with apoptosis induction (18,19). The WA-mediated inhibition of experimental metastasis in mice and invasion/migration in vitro were also demonstrated (22,23).

The primary objective of the present study was to determine the efficacy of WA for prevention of breast cancer using a clinically relevant transgenic mouse model. Demonstration of in vivo efficacy

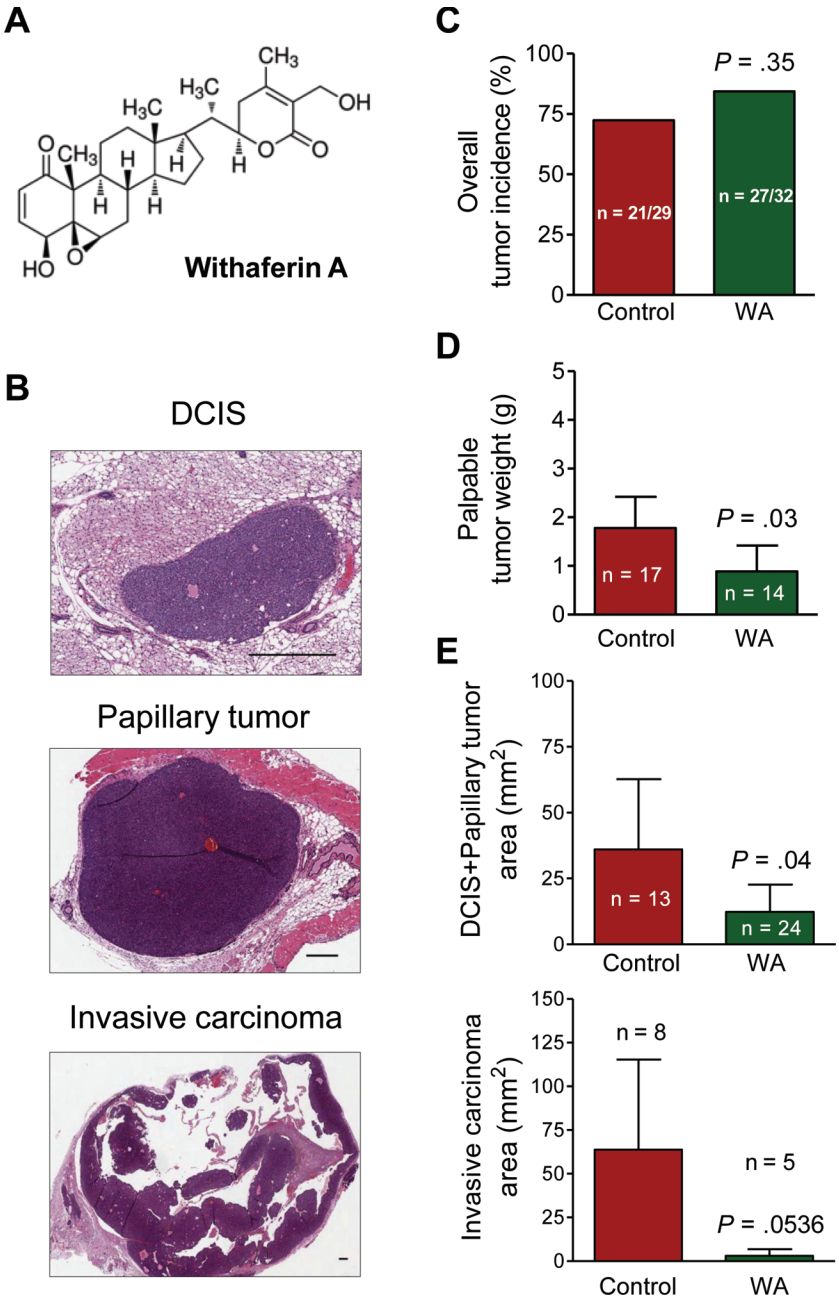

Figure 1. Withaferin A (WA) administration decreases burden of macroscopic (tumor size) and microscopic tumors (tumor area) in mouse mammary tumor virus–*neu* (MMTV-*neu*) transgenic mice. **A**) Chemical structure of WA. **B)** Representative hematoxylin and eosin–stained sections of mammary glands showing ductal carcinoma in situ (DCIS), papillary tumor, and focus of invasive carcinoma around papillary tumor (×50 magnification, scale bars = 400 μm). **C**) Overall tumor incidence in MMTV-*neu* mice of the WA treatment group and the control group. The *P* value was calculated by two-sided Fisher exact test. **D**) Macroscopic tumor burden. Results represent the mean weight of palpable tumors (macroscopic tumors) with a cutoff of ≥.05 g with corresponding 95% confidence intervals (**error bars**). Statistical significance of differences was determined by two-sided Student *t* test. **E)** Microscopic tumor burden (area) of DCIS plus papillary tumors and invasive carcinoma lesions. Results represent the mean areas of DCIS plus papillary tumors and invasive carcinoma with their corresponding 95% confidence intervals (**error bars**). Statistical significance of differences was determined by two-sided Student *t* test.

as well as safety and elucidation of the mechanisms underlying preventive effect against cancer are essential elements for the clinical development of promising cancer preventive agents. The impetus to determine the preventive effect of WA against breast cancer stemmed from the following observations: 1) viability of cultured human breast cancer cells was inhibited significantly in the presence of pharmacological doses of WA (19,21,22); 2) WA treatment suppressed several oncogenic pathways (23,24); and 3) WA administration retarded growth of MDA-MB-231 human breast cancer xenografts in athymic mice (19).

Materials and Methods

Reagents

Sources of reagents are described in the Supplementary Methods (available online).

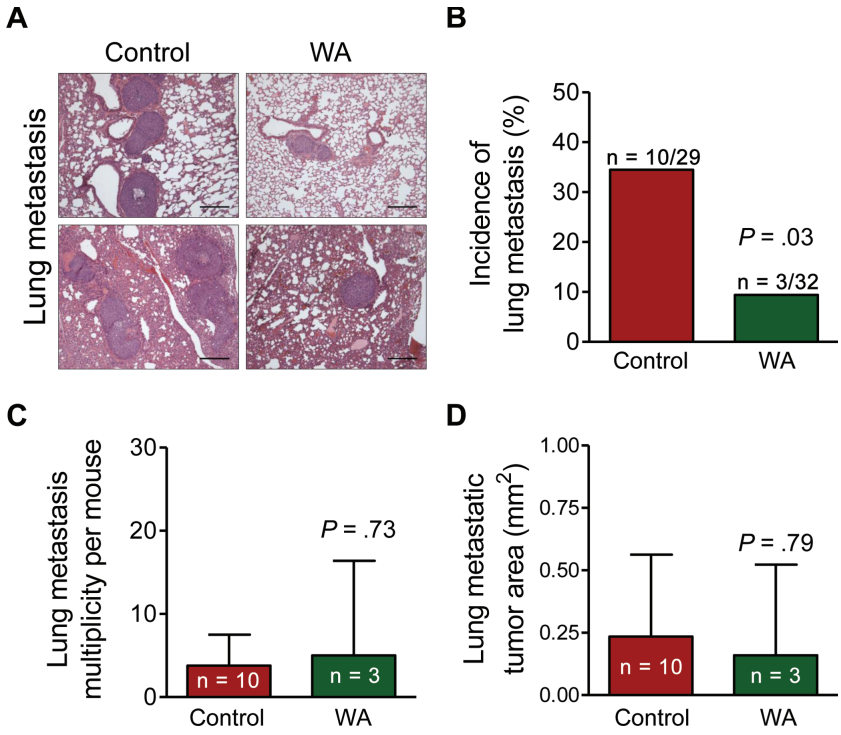

Figure 2. Withaferin A (WA) administration inhibits incidence of lung metastasis in mouse mammary tumor virus–*neu* mice. **A**) Representative hematoxylin and eosin–stained lung sections exhibiting metastasis in representative mice of the WA treatment group and the control group (×100 magnification, scale bars = 200 μm). **B**) Incidence of lung metastasis. Results shown are the percentages of mice with lung metastasis. The *P* value was calculated by two-sided Fisher exact test. **C**) Multiplicity of lung metastasis. Results show mean number of lung metastasis per mouse with 95% confidence intervals (**error bars**). Statistical significance of differences was determined by two-sided Student *t* test. **D**) Area of lung metastatic foci. Results represent the mean areas of lung metastatic tumor with their corresponding 95% confidence intervals (**error bars**). Statistical significance of differences was determined by two-sided Student *t* test.

Randomization and WA Administration

Use and care of mice for the study described herein was approved by and consistent with the guidelines of the Institutional Animal Care and Use Committee of the University of Pittsburgh. Four-week-old female mouse mammary tumor virus–*neu* (MMTV-*neu*) transgenic mice (homozygous; strain FVB/N-Tg [MMTV-*neu*] 202Mul/J) were purchased from the Jackson Laboratory (Bar Harbor, ME). Based on our previous work (25), we estimated that 28 mice per group would provide 80% power to detect a 40% difference in carcinoma incidence between groups at the .05 level of statistical significance. Initially, 60 mice were assigned to either vehicle-treated control arm (n = 30) or the WA treatment arm (n = 30). Four mice from the WA treatment group from one cage surprisingly died within a week after start of the treatment (after 2 or 3 intraperitoneal injections), which was unexpected based on our previous experience with athymic mice (19). The remaining mouse from this cage was sacrificed. Nevertheless, 10 mice were added to the WA treatment arm to account for this loss in sample size. Details of treatment are provided in the Supplementary Methods (available online). The dose and route of WA treatment were selected from the literature (18,19). One mouse from the control group was removed from the study due to excessive body weight loss (final number of evaluable mice in the control group, n = 29). Three mice from the WA treatment group were removed from the study/analysis due to morbidity, injection-related lump, or skin disorder (final number of evaluable mice in the WA treatment group, n = 32). Animal weight was recorded weekly. Mice were killed after 28 weeks of treatment by carbon dioxide euthanasia. Details of tissue collection, sectioning, and hematoxylin and eosin (H&E) staining, as well as pathological characteristics of ductal carcinoma in situ (DCIS), papillary tumors, and invasive carcinoma, are described in the Supplementary Methods (available online).

Immunohistochemical Analysis and Terminal Deoxynucleotidyl Transferase-Mediated Deoxyuridine-5′-Triphosphate Nick-End Labeling (TUNEL) Assay

Immunohistochemical analysis for various proteins and TUNEL assay were performed as described by us previously (26,27). Details of immunohistochemistry and TUNEL assay are included in the Supplementary Methods (available online).

Measurement of Complex III and Complex IV Activity

Activity of complex III (coenzyme Q:cytochrome *c* oxidoreductase or cytochrome bc_1 complex) and complex IV (cytochrome *c* oxidase) in tumor tissue lysate was measured as described by us previously for cells (21). Detailed methodology is included in the Supplementary Methods (available online).

Metabolomics

Plasma and tumor samples from eight different mice of each group were randomly selected and outsourced to Metabolon,

Inc (Durham, NC) for metabolic profiling. These samples were selected prior to the microscopic analysis of tumor incidence and burden. Details of the sample preparation, platforms used for metabolomics, and data analysis are described in the Supplementary Methods (available online).

Two-Dimensional Gel Electrophoresis and Mass Spectrometry

Tumor tissues from three different mice of each group were randomly selected and used to determine treatment-related protein alterations by two-dimensional gel electrophoresis followed by matrix-assisted laser desorption ionization-time of flight/time of flight (MALDI-TOF/TOF) (Applied Biomics, Hayward, CA) as described by us previously (26,27). Similar to metabolic profiling, these samples were selected prior to the microscopic analysis of tumor incidence and burden. Detailed methodology for proteomics and cluster analysis is included in the Supplementary Methods (available online).

Statistical Analyses

All statistical tests were two-sided. Statistical significance of difference in the incidence of mammary tumor and pulmonary metastasis was determined by two-sided Fisher exact test. Statistical significance of differences in other measured variables was determined by two-sided Student *t* test. All statistical tests were done using GraphPad Prism version 4.03 software (La Jolla, CA). The *P* values are rounded to the second or third significant digit. Exact *P* value (no rounding) is shown if it is very close to the .05 level. Difference was considered significant at *P* less than or equal to .05.

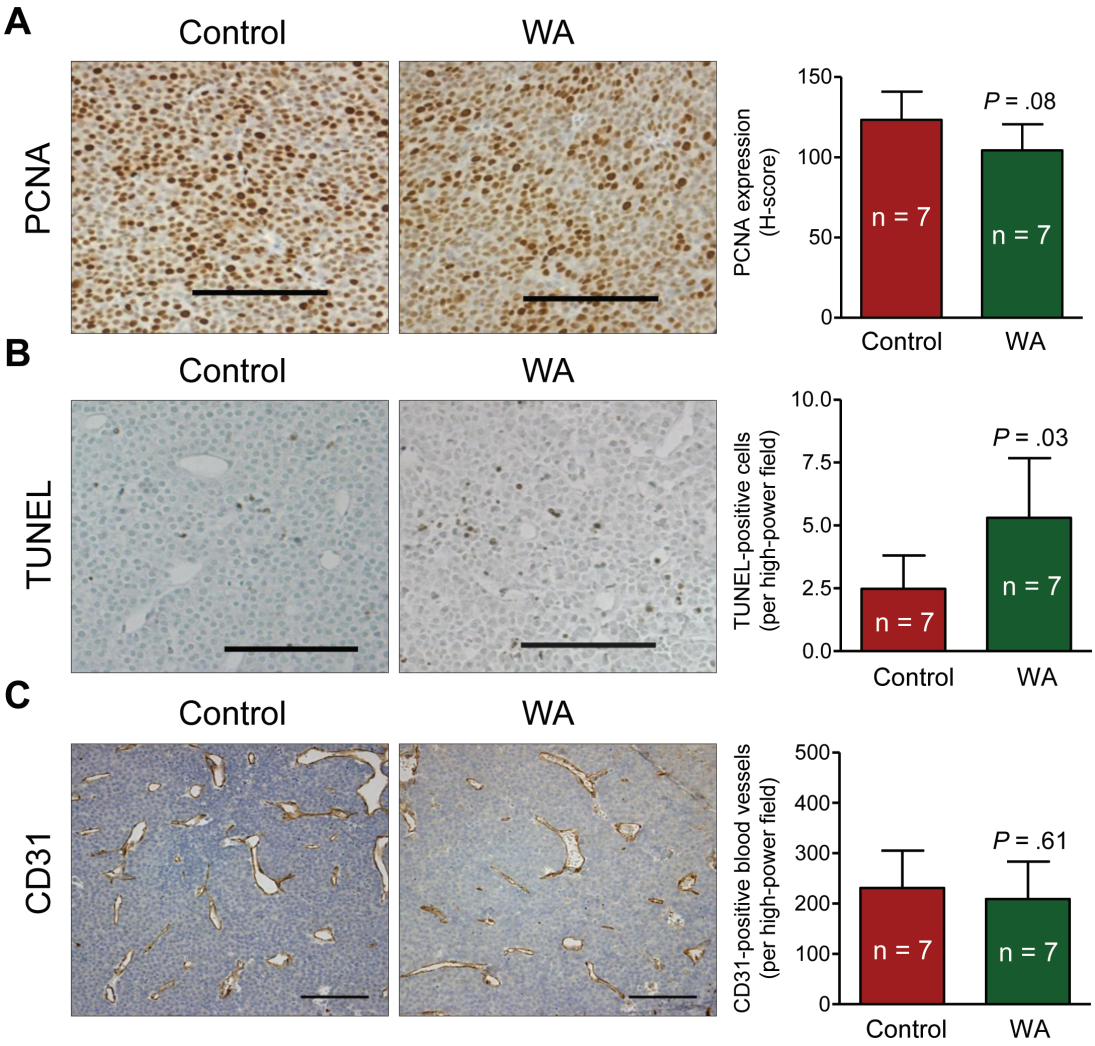

Figure 3. Withaferin A (WA) administration results in apoptosis induction in the tumor of mouse mammary tumor virus–*neu* mice. **A**) Proliferating cell nuclear antigen (PCNA) expression revealing cell proliferation in representative tumor of a mouse from the WA treatment group and the control group. Immunohistochemical staining was performed with anti-PCNA antibody and analyzed by nuclear algorithm using Aperio ImageScope software (×200 magnification, scale bars = 100 μm). Results shown are mean H-score for PCNA expression with their 95% confidence intervals (**error bars**, n = 7). **B**) Terminal deoxynucleotidyl transferase-mediated deoxyuridine-5′-triphosphate nick-end labeling (TUNEL)–positive apoptotic cells in representative tumor of a mouse from the WA treatment group and the control group. Apoptotic cells were visualized by TUNEL staining and analyzed by nuclear algorithm using Aperio ImageScope software (×200 magnification, scale bars = 100 μm). Results represent mean TUNEL-positive cells per high-power field (n = 7) with their 95% confidence intervals (**error bars**). **C**) CD31-positive blood vessels in representative tumor of a mouse from the WA treatment group and the control group. Immunohistochemical staining was performed with anti-CD31 antibody and quantified using Image ProPlus 5.0 software (×200 magnification, scale bars = 100 μm). Results represent mean CD31-positive cells per high-power field (n = 7) with their 95% confidence intervals (**error bars**). Statistical significance of differences was determined by two-sided Student *t* test (**A**–**C**).

Results

Effect of WA Treatment on Mammary Cancer Development in MMTV-*neu* Mice

We used a mouse model (MMTV-*neu*), which faithfully recapitulates aspects of human disease progression in a subset of women with breast cancer (28–30), to determine preventive efficacy of WA. The mean initial and final body weights of the control and WA-treated mice were comparable (results not shown). Pathological features of DCIS, papillary tumor, and invasive carcinoma are shown in Figure 1B. The overall mammary tumor incidence was slightly higher in the WA treatment group (84.38%) compared with the control group (72.41%), but the difference was not statistically significant (P = .35 by Fisher exact test) (Figure 1C). On the other hand, mean palpable (macroscopic) tumor weight in the WA treatment group (range = .07–2.87 g) was lower by 50% in comparison with the control group (range = .05–4.51 g) (mean = .89 vs 1.78 g, respectively; difference = –.89 g; 95% confidence interval [CI] = –1.71 g to –.07 g; P = .03 by two-sided Student t test) (Figure 1D). The mean tumor weight was calculated from sum of tumor weight in an animal, and the average of tumor weight over all the animals for each group. Furthermore, microscopic examination of the H&E-stained mammary gland sections from each mouse of both groups revealed a decrease in the area (burden) of DCIS plus papillary tumors as well as invasive carcinoma in the WA group compared with the control group (Figure 1E). For example, the mean area of invasive carcinoma was lower by 95.14% in the WA

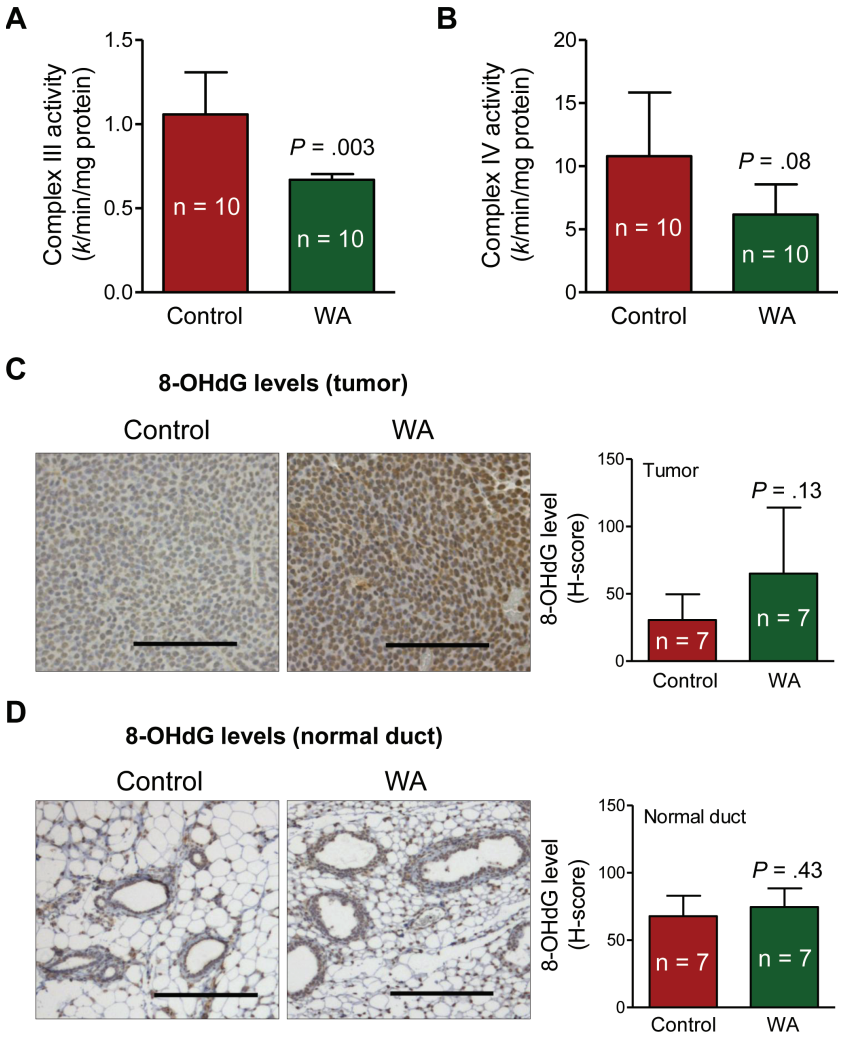

Figure 4. Withaferin A (WA) administration inhibits activity of complex III in the tumor of mouse mammary tumor virus–*neu* mice. **A)** Activity of complex III in tumor lysates from mice of the WA treatment group and the control group. Complex III activity was measured using oxidized cytochrome *c* and ubiquinol as substrates. Results represent mean complex III activity (n = 10) with their 95% confidence intervals (**error bars**). **B**) Activity of complex IV in tumor lysates from mice of the WA treatment group and the control group. Complex IV activity was measured using reduced cytochrome *c* as the substrate. Results represent mean complex IV activity (n = 10) with their 95% confidence intervals (**error bars**). **C)** 8-Hydroxy-2′-deoxyguanosine (8-OHdG) level by immunohistochemistry in representative tumors of a mouse from the WA treatment group and the control group. Immunohistochemical staining was performed with anti-8-OHdG antibody and analyzed by nuclear algorithm using Aperio ImageScope software (×200 magnification, scale bars = 100 μm). Bar graph shows mean H-score for 8-OHdG (n = 7) with their 95% confidence intervals (**error bars**). **D**) 8-OHdG level by immunohistochemistry in representative normal mammary ducts of a mouse from the WA treatment group and the control group. Immunohistochemical staining was performed with anti-8-OHdG antibody and analyzed by nuclear algorithm using Aperio ImageScope software (×200 magnification, scale bars = 100 μm). Bar graph shows mean H-score for 8-OHdG (n = 7) with their 95% confidence intervals (**error bars**). Statistical significance of differences was determined by two-sided Student *t* test (**A**–**D**).

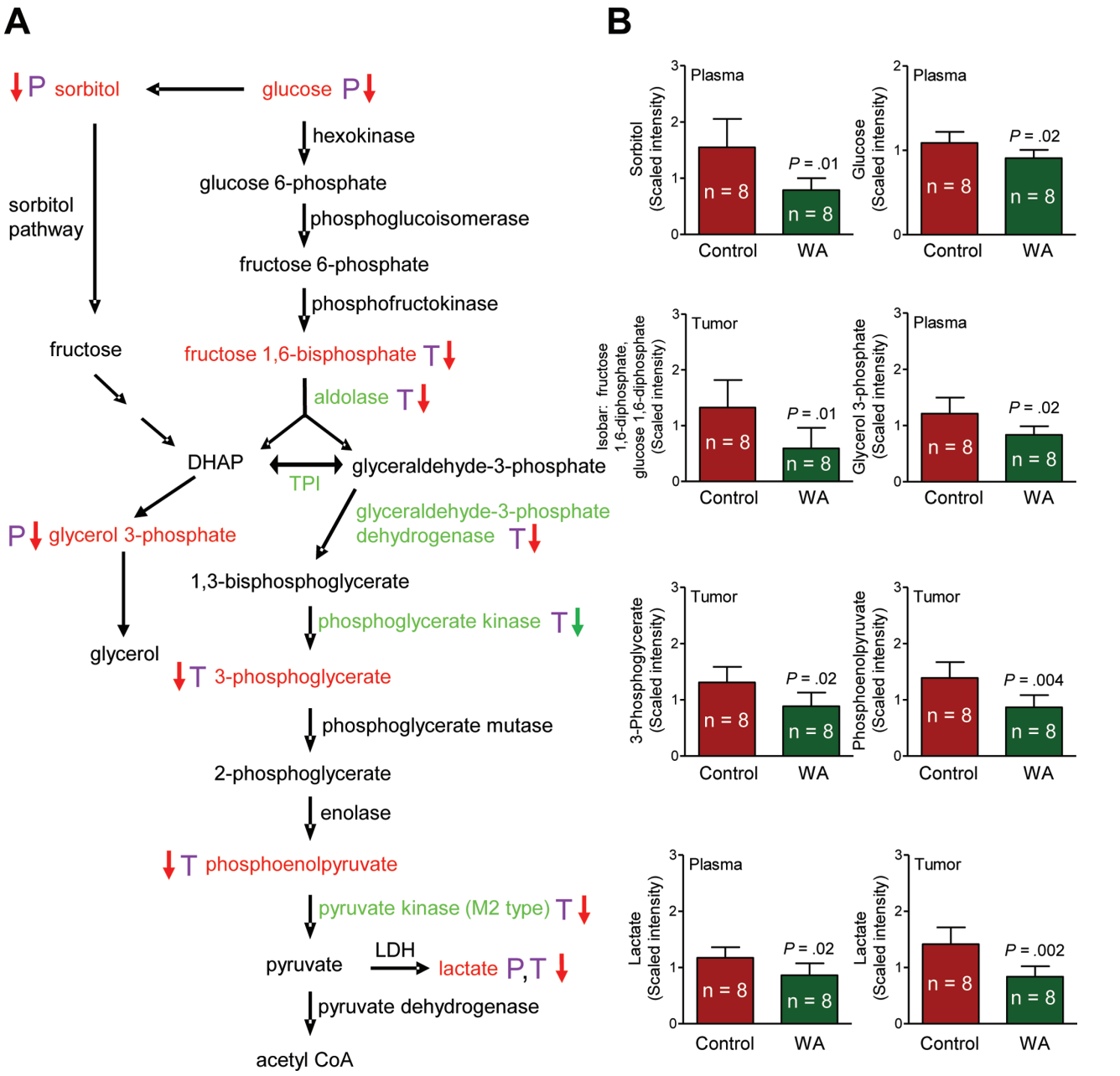

Figure 5. Withaferin A (WA)–mediated alterations in levels of glycolysis intermediates in the plasma and tumor of mouse mammary tumor virus-*neu* mice. **A)** Glycolysis pathway. **B)** Levels of glycolysis intermediates in plasma and/or tumors of mice from the WA treatment group and the control group. Plasma and tumor samples from eight different mice of each group were outsourced to Metabolon, Inc (Durham, NC) for metabolic profiling. The letters P (**purple**) and T (**purple**) represent plasma and tumor, respectively. A **red arrow** denotes *P* less than .05, and a green arrow denotes *P* greater than or equal to .05 and *P* less than .10. Glycolysis intermediates with significant differences between the WA treatment group and the control group are indicated with **red font**. Glycolysis-related proteins with significant differences in expression between the WA treatment group and the control group are indicated with **green font**. **Bar graphs** represent the mean scaled intensity of the intermediates (n = 8) with their 95% confidence intervals (**error bars**) acetyl CoA = acetyl coenzyme A; DHAP = dihydroxyacetone phosphate; LDH = lactate dehydrogenase; TPI = triose phosphate isomerase.

group compared with the control group (mean = 3.10 vs 63.77 mm^2, respectively; difference = –60.67 mm^2; 95% CI = –122.50 mm^2 to 1.13 mm^2; *P* = .0536 by two-sided Student *t* test) (Figure 1E). These results indicated that WA administration resulted in inhibition of mammary tumor progression in the MMTV-*neu* mouse model without any signs of treatment-related toxicity except for the unexpected deaths confined to a single cage and removal of 3 mice from the study/analysis due to morbidity, injection-related lump, or skin sores throughout the body.

Effect of WA Treatment on Lung Metastasis

Figure 2A shows H&E-stained lung sections from two representative mice each of WA group and control group. Incidence of lung metastasis was lower by 72.80% in the WA group in comparison with the control group (mean = 9.38% vs 34.48%, respectively; difference = –25.10%; 95% CI of the difference could not be determined due to low incidence in the WA treatment group [n = 3]; *P* = .03 by two-sided Fisher exact test) (Figure 2B). In contrast, the lung metastasis multiplicity per mouse (Figure 2C) or the lung

metastatic tumor area (Figure 2D) did not differ between the two groups.

Effect of WA Treatment on Tumor Apoptosis

Because the size of the microscopic tumors was rather small in the mammary glands of many mice of the WA treatment group, immunohistochemical analysis was not possible for every sample. Nevertheless, we used randomly selected mammary gland sections from seven mice in each group for immunohistochemical analysis of human epidermal growth factor receptor 2 (HER-2) and proliferation marker proliferating cell nuclear antigen (PCNA) (31). Expression of HER-2 did not differ statistically significantly between tumors of mice from the WA treatment group and the control group (results not shown). Likewise, the difference in mean H-score for nuclear PCNA expression in the tumors of mice from the WA treatment group and the control group was not statistically significant (Figure 3A). The mean number of TUNEL-positive cells per high-power field in the tumors of mice from the WA group was higher by 2.14-fold compared with those of the control group (mean = 5.30 vs 2.48 TUNEL-positive cells/high-power field, respectively; difference = 2.82; 95% CI = .40 to 5.25; P = .03 by two-sided Student t test, n = 7) (Figure 3B). We next proceeded to determine the in vivo effect of WA administration on formation of new blood vessels (neoangiogenesis) in the tumor because 1) neoangiogenesis is essential for tumor growth as well as metastatic spread (32); and 2) WA was previously shown to inhibit angiogenesis in vitro (33). The number of CD31-positive blood vessels in the tumors of mice from the WA treatment group and the control group was similar (Figure 3C).

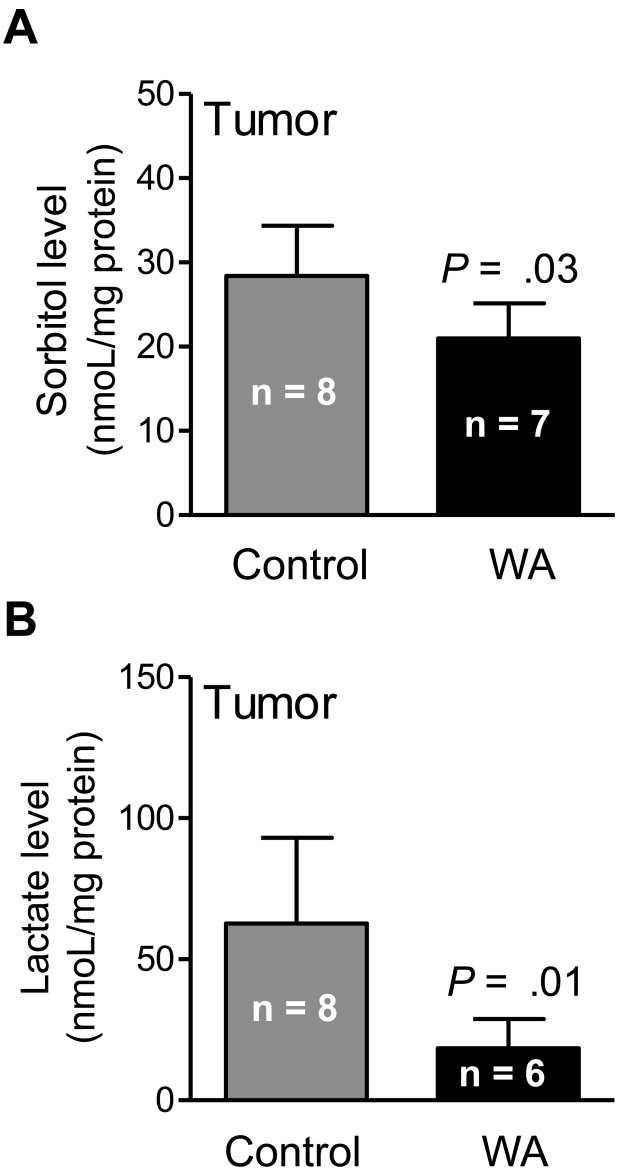

Figure 6. Sorbitol and lactate levels in tumors of mouse mammary tumor virus-*neu* mice from the withaferin A (WA) treatment group and the control group. Results shown are means and their 95% confidence intervals (**error bars**). Statistical significance of differences was determined by two-sided Student t test.

Effect of WA Treatment on Tumor Complex III Activity

Molecular circuitry of WA-induced apoptosis in cultured breast cancer cells involves inhibition of complex III of the mitochondrial respiratory chain leading to production of reactive oxygen species and eventual cell death (21). As shown in Figure 4A, mean complex III activity in tumors from mice in the WA group was lower by 36.79% than in the tumor of mice from the control group (mean = .67 vs 1.06 k/min/mg protein, respectively; difference = –.39; 95% CI = –.62 to –.15; P = .003 by two-sided Student t test; n = 10) (Figure 4A). Mean activity of complex IV in the tumors from mice of WA group was also lower by 42.78% than in the tumors of mice from the control group, but the difference was not statistically significant (Figure 4B). We performed immunohistochemistry for 8-hydroxy-2′-deoxyguanosine (8-OHdG) levels to assess oxidative stress in the tumor as well as in the normal mammary ducts. The 8-OHdG is a product of oxidatively damaged DNA formed by hydroxyl radicals. The mean H-score for 8-OHdG in the tumors from mice of the WA treatment group was higher by 2.13-fold than in the tumors from mice of the control group, but the difference was not statistically significant due to large data scatter, especially in the WA treatment samples (Figure 4C). Nevertheless, a majority of the tumors from mice in the WA treatment group exhibited increased staining for 8-OHdG compared with the tumors from mice in the control group. This trend was not discernible in the normal mammary ducts (Figure 4D). In summary, these observations provided in vivo evidence for WA-mediated inhibition of complex III activity.

Metabolic Alterations Associated With Mammary Cancer Prevention by WA

A total of 320 and 328 biochemicals of known identity were detectable in the plasma and tumor tissues, respectively. The WA-mediated mammary cancer prevention was associated with a statistically significant alteration at the $P \leq .05$ level in 76 biochemicals in the plasma, with increases observed for 24 metabolites and decreases observed for 52 metabolites. Metabolomics using tumor tissues revealed alterations in 24 biochemicals at the P less than or equal to .05 level (n = 2 increase, n = 22 decrease) upon WA administration. One change that was highly consistent in the plasma and tumor tissues from mice of the WA treatment group compared with those from the control group was a decrease in glucose utilization and glycolysis

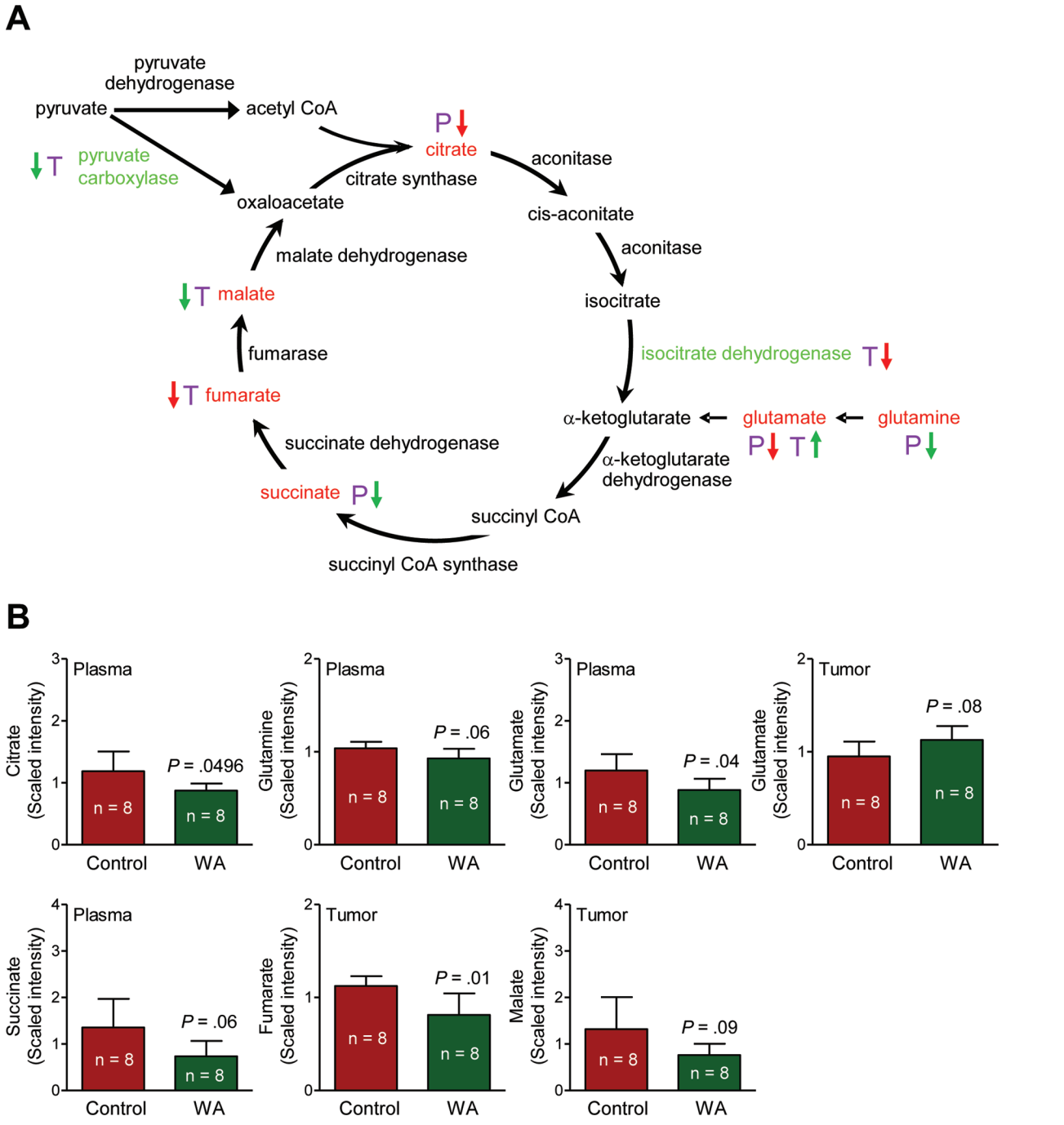

Figure 7. Withaferin A (WA)–mediated alterations in the levels of tricarboxylic acid (TCA) cycle intermediates in the plasma and/or tumor of mouse mammary tumor virus-*neu* mice. **A)** TCA cycle. **B)** Levels of TCA cycle intermediates in plasma and/or tumors of mice from the WA treatment group and the control group. Plasma and tumor samples from 8 different mice of each group were outsourced to Metabolon (Durham, NC) for metabolic profiling. The letters P (**purple**) and T (**purple**) represent plasma and tumor, respectively. A **red arrow** denotes *P* less than .05, and a **green arrow** denotes *P* greater than or equal to .05 and *P* less than .10. TCA cycle intermediates with differences between the WA treatment group and the control group are indicated with **red font**. TCA cycle–related proteins with differences in expression between the WA treatment group and the control group are indicated with **green font**. **Bar graphs** represent the mean scaled intensity of the intermediates (n = 8) with their 95% confidence intervals (**error bars**). acetyl CoA = acetyl coenzyme A; succinyl CoA = succinyl conenzyme A; succinyl CoA synthase = succinyl coenzyme A synthase.

and tricarboxylic acid (TCA) cycle intermediates. A complete list of the metabolite level differences in the plasma and tumor tissues between mice of the WA treatment group and the control group can be found in Supplementary Table 1 (available online). Figure 5A shows the glycolysis pathway and the changes in glycolysis-related intermediates (biochemicals highlighted with red font in Figure 5A). For example, the level of lactate was statistically significantly lower in tumors of WA-treated mice compared with control (mean = .84 vs 1.42 scaled intensity, respectively; difference = –.58; 95% CI = –.90 to –.26; P = .002 by two-sided Student t test; n = 8) (Figure 5B). Suppression of sorbitol and lactate in the tumor of WA-treated mice was confirmed by measurement of their levels (Figure 6, A and B).

Table 1. Identification of altered proteins in the tumors of mouse mammary tumor virus–*neu* (MMTV-*neu*) mice in response to withaferin A treatment

Protein name	Master No.	Protein ID	Average ratio, withaferin A/control*	*P*†
Upregulation				
Matr3 [Mus musculus]	165	2	1.4	.08
Gelsolin isoform 2 [Mus musculus]	312	4	2.0	.07
Moesin [Mus musculus]	444	5	1.4	.08
Acyl-Coenzyme A dehydrogenase, very long chain [Mus musculus]	551	7	1.4	.07
Sorting and assembly machinery component 50 homolog [Mus musculus]	741	9	1.6	.02
Protein synthesis initiation factor 4A [Mus musculus]	900	11	1.4	.06
Alpha-fetoprotein [Mus musculus]	1066	12	1.8	.08
Annexin A1 [Mus musculus]	1134	20	1.4	.04
Annexin A2 [Mus musculus]	1173	21	1.3	.08
Anxa5 protein [Mus musculus]	1302	24	1.4	.09
Put. β-actin (aa 27–375) [Mus musculus]	1328	27	2.6	.10
Protein disulfide-isomerase A3 precursor [Mus musculus]	1341	29	2.5	.07
Enoyl-CoA hydratase domain-containing protein 1 isoform b [Mus musculus]	1306	30	2.6	.07
Esterase D/formylglutathione hydrolase, isoform CRA_b [Mus musculus]	1310	31	1.3	.02
U2 small nuclear ribonucleoprotein A′ [Mus musculus]	1482	32	2.4	.07
Sepiapterin reductase [Mus musculus]	1580	33	1.5	.08
NADH dehydrogenase (ubiquinone) Fe-S protein 3 [Mus musculus]	1590	34	2.8	.08
Rexo2 protein [Mus musculus]	1624	35	1.6	.001
Growth factor receptor bound protein 2 [Mus musculus]	1628	36	1.6	.07
Proteasome subunit beta type-3 [Mus musculus]	1650	37	1.5	.01
Triosephosphate isomerase [Mus musculus]‡	1675	39	1.3	.09
RIKEN cDNA 0610011F06, isoform CRA_b [Mus musculus]	1695	40	2.5	.09
RecName: Full=UMP-CMP kinase; AltName:Full=Cytidine monophosphate kinase; AltName: Full=Cytidylate	1711	41	1.5	.08
Ferritin light chain 2 [Mus musculus]	1731	42	3.5	.06
GTP-binding protein SAR1a [Mus musculus]	1715	43	1.5	.01
Cell division control protein 42 homolog isoform 1 [Homo sapiens]	1756	44	1.5	.02
Chain A, Recombinant Mouse L-Chain Ferritin	1755	45	1.6	.01
Alpha-S2-casein-like A precursor [Mus musculus]	1803	46	4.4	.10
Vacuolar protein sorting-associated protein 29 [Mus musculus]	1804	47	1.3	.01
Vacuolar protein-sorting-associated protein 25 [Mus musculus]	1871	48	1.9	.03
Ferritin heavy chain [Mus musculus]‡	1800	49	2.0	.02
Ferritin heavy chain [Mus musculus]‡	1795	50	2.5	.07
c-Myc-binding protein [Mus musculus]	2411	65	1.3	.09
Downregulation				
Damage-specific DNA binding protein 1 [Mus musculus]	168	1	–1.4	.003
Pyruvate carboxylase, mitochondrial isoform 2 [Mus musculus]	175	3	–1.4	.06
Transketolase [Mus musculus]	540	6	–1.3	.01
M2-type pyruvate kinase [Mus musculus]	640	8	–1.4	.04
Calreticulin precursor [Mus musculus]	742	10	–1.4	.003
Isocitrate dehydrogenase 1 (NADP+), soluble [Mus musculus]	944	13	–1.3	.003
Phosphoglycerate kinase [Mus musculus]	969	14	–1.5	.06
Creatine kinase U-type, mitochondrial precursor [Mus musculus]	1003	15	–2.1	.09
Acetyl-CoA acetyltransferase, mitochondrial precursor [Mus musculus]	1026	16	–1.5	.09
Fructose-bisphosphate aldolase A isoform 2 [Mus musculus]‡	1041	17	–1.7	.03
Fructose-bisphosphate aldolase A isoform 2 [Mus musculus]‡	1038	18	–1.7	.02
Phosphoserine aminotransferase isoform 2 [Mus musculus]	1109	19	–1.4	.02
Glyceraldehyde-3-phosphate dehydrogenase [Mus musculus]	1184	22	–1.8	.045
Heterogeneous nuclear ribonucleoproteins A2/B1 isoform 1 [Mus musculus]	1255	23	–1.3	.08
Eukaryotic translation elongation factor 1 beta 2 [Mus musculus]	1419	25	–1.4	.02
Impa1 protein [Mus musculus]	1368	26	–1.4	.01
Proteasome activator PA28 beta subunit [Mus musculus]	1407	28	–1.3	.01
Triosephosphate isomerase [Mus musculus]‡	1609	38	–1.6	.06
Myosin light chain, regulatory B-like [Mus musculus]‡	1864	51	–1.9	.01
Myosin light chain, regulatory B-like [Mus musculus]‡	1860	52	–1.6	.01
Neurocalcin-delta [Bos taurus]	1955	53	–1.7	.04
Bis(5′-nucleosyl)-tetraphosphatase [asymmetrical] [Mus musculus]	2134	54	–2.5	.01
PREDICTED: peptidyl-prolyl cis-trans isomerase A-like [Mus musculus]‡	2138	55	–2.2	.004
Tumor metastatic process-associated protein NM23 [Mus musculus]	2200	56	–1.7	.02

(Table continues)

Table 1 (Continued).

Protein name	Master No.	Protein ID	Average ratio, withaferin A/control*	*P*†
Nucleoside diphosphate kinase B [Mus musculus]	2124	57	–1.4	.06
PREDICTED: peptidyl-prolyl cis-trans isomerase A-like [Mus musculus]‡	2175	58	–1.5	.001
PREDICTED: peptidyl-prolyl cis-trans isomerase A-like [Mus musculus]‡	2154	59	–1.6	.01
PREDICTED: peptidyl-prolyl cis-trans isomerase A-like [Mus musculus]‡	2182	60	–1.4	.01
Destrin [Mus musculus]‡	2118	61	–1.5	.07
Destrin [Mus musculus]‡	2129	62	–3.1	.03
Peroxisomal membrane protein 20 [Mus musculus]	2204	63	–2.1	.01
Myosin light polypeptide 6 [Mus musculus]	2239	64	–1.5	.001

* Randomly selected tumor specimens from three mice in each group were used for proteomics analysis.

† All *P* values were calculated by a two-sided Student *t* test.

‡ The protein spots likely represent isoforms or posttranslational modification(s) of the same protein.

In addition, reduced levels of many TCA cycle intermediates in the plasma or tumor tissue was also found to be associated with WA-mediated mammary cancer prevention (Figure 7, A and B; altered metabolites are highlighted with red font in Figure 7A). Other altered biochemicals were reflective of changes in arginine metabolism, polyamine biosynthesis pathway, glutathione metabolism, lipid metabolism, and catabolism of branched-chain amino acids (Supplementary Table 1, available online).

Tumor Protein Expression Changes Associated With Mammary Cancer Prevention by WA

Proteomics confirmed downregulation of many glycolysis- and TCA-cycle related proteins in the tumor from mice in the WA treatment group in comparison with that of the control group (Table 1, Figures 5A and 7A; protein changes are indicated with green font). Cluster analysis revealed statistically significant enrichment of gluconeogenesis/glycolysis and annexin proteins (Supplementary Table 2, available online).

Discussion

This study demonstrates that a very mild regimen of WA administration involving three intraperitoneal injections per week results in statistically significant inhibition of mammary cancer burden and pulmonary metastasis incidence in the MMTV-*neu* mouse model. The WA-mediated prevention of mammary cancer is associated with increased apoptosis. This study also provides in vivo confirmation of the previous cellular mechanistic observations (21). Consistent with in vitro observations in cultured breast cancer cells (21), the apoptosis induction by WA administration in vivo is associated with a significant decrease in the activity of complex III. Relatively higher levels of 8-OHdG in tumor from WA-treated mice compared with that of control mice further attest to the in vivo contribution of the reactive oxygen species–dependent apoptosis mechanism to the cancer-preventive effect of WA.

This study indicates that WA administration inhibits tumor burden but not tumor incidence. A few possibilities deserve attention to explain these results. First, it is possible that inhibition of mammary cancer incidence by WA requires daily administration of the agent rather than the intermittent dosing schedule employed in this study. Second, we have shown recently that WA treatment causes activation of Notch2 and Notch4 in cultured human breast cancer cells (22). Thus, it is also plausible that the activation of Notch signaling, which is often hyperactive in human breast cancers (34,35), impedes preventive efficacy of WA. However, additional work is needed to systematically explore these possibilities.

Increased uptake of glucose and dependence on glycolysis instead of oxidative phosphorylation are biochemical hallmarks of cancer cells initially observed by Otto Warburg several decades ago (36). Increased glycolysis confers survival advantage to cancer cells and is linked to oncogenic transformation (37,38). More recent studies have indicated that hypoxic tumor cells primarily use glucose for glycolytic energy production and release lactic acid that fuels the oxidative metabolism in oxygenated tumor cells (39). The metabolomic and proteomic results described herein show, for the first time, that mammary cancer prevention by WA is associated with suppression of glycolysis and TCA cycle, at least in the MMTV-*neu* mice.

Many glycolysis- and TCA cycle–related proteins downregulated in the tumors of WA-treated mice have relevance to breast cancer (40–46). For example, fructose-bisphosphate aldolase and glyceraldehyde-3-phosphate dehydrogenase, both of which are significantly downregulated in tumors from WA-treated mice, are overexpressed in ductal carcinoma compared with normal breast tissue (40). Protein alteration profiling in infiltrating ductal carcinoma of the breast from Tunisian women revealed overexpression of several glycolysis-related enzymes including phosphoglycerate kinase (41). The tumors from the WA-treated mice show decreased expression of M2-type pyruvate kinase, which is considered an attractive target for cancer therapy (44). Breast cancer relevance has also been suggested for the TCA cycle–related enzyme isocitrate dehydrogenase (45), whose expression is significantly decreased in the tumors of WA-treated mice.

Our study has some limitations. First, it is important to determine oral bioavailability of WA as other routes of administrations are not practical for cancer prevention purposes. Second, detailed toxicology of WA is needed to determine its safety in light of unexpected deaths from this group, albeit confined to a single cage. Third, it remains to be determined if the WA-mediated metabolic alterations observed in the present study are unique to the HER-2–driven cancer model. Finally, the functional relevance of other altered proteins in the context of WA-mediated prevention of breast tumor is unclear.

References

1. Jemal A, Siegel R, Xu J, Ward E. Cancer statistics, 2010. *CA Cancer J Clin*. 2010;60(5):277–300.
2. Fisher B, Costantino JP, Wickerham DL, et al. Tamoxifen for prevention of breast cancer: report of the National Surgical Adjuvant Breast and Bowel Project P-1 Study. *J Natl Cancer Inst*. 1998;90(18):1371–1388.
3. Cauley JA, Norton L, Lippman ME, et al. Continued breast cancer risk reduction in postmenopausal women treated with raloxifene: 4-year results from the MORE trial. *Breast Cancer Res Treat*. 2001;65(2):125–134.
4. Goss PE, Ingle JN, Alés-Martínez JE, et al. Exemestane for breast-cancer prevention in postmenopausal women. *N Engl J Med*. 2011;364 (25):2381–2391.
5. Obiorah I, Jordan VC. Progress in endocrine approaches to the treatment and prevention of breast cancer. *Maturitas*. 2011;70(4):315–321.
6. Boccardo F, Rubagotti A, Guglielmini P, et al. Switching to anastrozole versus continued tamoxifen treatment of early breast cancer. Updated results of the Italian tamoxifen anastrozole (ITA) trial. *Ann Oncol*. 2006;17(suppl 7):vii10–vii14.
7. Garodia P, Ichikawa H, Malani N, Sethi G, Aggarwal BB. From ancient medicine to modern medicine: Ayurvedic concepts of health and their role in inflammation and cancer. *J Soc Integr Oncol*. 2007;5(1):25–37.
8. Gupta SK, Mohanty I, Talwar KK, et al. Cardioprotection from ischemia and reperfusion injury by *Withania somnifera*: a hemodynamic, biochemical and histopathological assessment. *Mol Cell Biochem*. 2004;260(1–2):39–47.
9. Ahmad M, Saleem S, Ahmad AS, et al. Neuroprotective effects of *Withania somnifera* on 6-hydroxydopamine induced parkinsonism in rats. *Hum Exp Toxicol*. 2005;24(3):137–147.
10. Panda S, Kar A. Changes in thyroid hormone concentrations after administration of ashwagandha root extract to adult male mice. *J Pharm Pharmacol*. 1998;50(9):1065–1068.
11. Owais M, Sharad KS, Shehbaz A, Saleemuddin M. Antibacterial efficacy of *Withania somnifera* (ashwagandha) an indigenous medicinal plant against experimental murine salmonellosis. *Phytomedicine*. 2005;12(3):229–235.
12. Rasool M, Varalakshmi P. Immunomodulatory role of *Withania somnifera* root powder on experimental induced inflammation: an in vivo and in vitro study. *Vascul Pharmacol*. 2006;44(6):406–410.
13. Devi PU, Sharada AC, Solomon FE. Antitumor and radiosensitizing effects of *Withania somnifera* (ashwagandha) on a transplantable mouse tumor, Sarcoma-180. *Indian J Exp Biol*. 1993;31(7):607–611.
14. Widodo N, Kaur K, Shrestha BG, et al. Selective killing of cancer cells by leaf extract of ashwagandha: identification of a tumor-inhibitory factor and the first molecular insights to its effect. *Clin Cancer Res*. 2007;13(7):2298–2306.
15. Shohat B, Joshua H. Effect of withaferin A on Ehrlich ascites tumor cells. II. Target tumor cell destruction in vivo by immune activation. *Int J Cancer*. 1971;8(3):487–496.
16. Devi PU, Kamath R, Rao BS. Radiosensitization of a mouse melanoma by withaferin A: in vivo studies. *Indian J Exp Biol*. 2000;38(5):432–437.
17. Manoharan S, Panjamurthy K, Menon VP, Balakrishnan S, Alias LM. Protective effect of withaferin-A on tumour formation in 7,12-dimethylbenz[a]anthracene induced oral carcinogenesis in hamsters. *Indian J Exp Biol*. 2009;47(1):16–23.
18. Srinivasan S, Ranga RS, Burikhanov R, Han SS, Chendil D. Par-4-dependent apoptosis by the dietary compound withaferin A in prostate cancer cells. *Cancer Res*. 2007;67(1):246–253.
19. Stan SD, Hahm ER, Warin R, Singh SV. Withaferin A causes FOXO3a- and Bim-dependent apoptosis and inhibits growth of human breast cancer cells in vivo. *Cancer Res*. 2008;68(18):7661–7669.
20. Thaiparambil JT, Bender L, Ganesh T, et al. Withaferin A inhibits breast cancer invasion and metastasis at sub-cytotoxic doses by inducing vimentin disassembly and serine 56 phosphorylation. *Int J Cancer*. 2011;129(11):2744–2755.
21. Hahm ER, Moura MB, Kelley EE, Van Houten B, Shiva S, Singh SV. Withaferin A-induced apoptosis in human breast cancer cells is mediated by reactive oxygen species. *PLoS One*. 2011;6(8):e23354.
22. Lee J, Sehrawat A, Singh SV. Withaferin A causes activation of Notch2 and Notch4 in human breast cancer cells. *Breast Cancer Res Treat*. 2012;136(1):45–56.
23. Lee J, Hahm ER, Singh SV. Withaferin A inhibits activation of signal transducer and activator of transcription 3 in human breast cancer cells. *Carcinogenesis*. 2010;31(11):1991–1998.
24. Hahm ER, Lee J, Huang Y, Singh SV. Withaferin A suppresses estrogen receptor-α expression in human breast cancer cells. *Mol Carcinog*. 2011;50(8):614–624.
25. Warin R, Chambers WH, Potter DM, Singh SV. Prevention of mammary carcinogenesis in MMTV-*neu* mice by cruciferous vegetable constituent benzyl isothiocyanate. *Cancer Res*. 2009;69(24):9473–9480.
26. Powolny AA, Bommareddy A, Hahm ER, et al. Chemopreventative potential of the cruciferous vegetable constituent phenethyl isothiocyanate in a mouse model of prostate cancer. *J Natl Cancer Inst*. 2011;103(7):571–584.
27. Singh SV, Kim SH, Sehrawat A, et al. Biomarkers of phenethyl isothiocyanate-mediated mammary cancer chemoprevention in a clinically relevant mouse model. *J Natl Cancer Inst*. 2012;104(16):1228–1239.
28. Slamon DJ, Clark GM, Wong SG, Levin WJ, Ullrich A, McGuire WL. Human breast cancer: correlation of relapse and survival with amplification of the HER-2/neu oncogene. *Science*. 1987;235(4785):177–182.
29. Guy CT, Webster MA, Schaller M, Parsons TJ, Cardiff RD, Muller WJ. Expression of the *neu* protooncogene in the mammary epithelium of transgenic mice induces metastatic disease. *Proc Natl Acad Sci U S A*. 1992;89(22):10578–10582.
30. Ménard S, Tagliabue E, Campiglio M, Pupa SM. Role of HER2 gene overexpression in breast carcinoma. *J Cell Physiol*. 2000;182(2):150–162.
31. Leonardi E, Girlando S, Serio G, et al. PCNA and Ki67 expression in breast carcinoma: correlations with clinical and biological variables. *J Clin Pathol*. 1992;45(5):416–419.
32. Folkman J. Tumor angiogenesis: therapeutic implications. *N Eng J Med*. 1971;285(21):1182–1186.
33. Mohan R, Hammers HJ, Bargagna-Mohan P, et al. Withaferin A is a potent inhibitor of angiogenesis. *Angiogenesis*. 2004;7(2):115–122.
34. Leong KG, Karsan A. Recent insights into the role of Notch signaling in tumorigenesis. *Blood*. 2006;107(6):2223–2233.
35. Rizzo P, Miao H, D'Souza G, et al. Cross-talk between notch and the estrogen receptor in breast cancer suggests novel therapeutic approaches. *Cancer Res*. 2008;68(13):5226–5235.
36. Warburg O. On the origin of cancer cells. *Science*. 1956;123:309–314.
37. EI Mjiyad N, Caro-Maldonado A, Ramírez-Peinado S, Muñoz-Pinedo C. Sugar-free approaches to cancer cell killing. *Oncogene*. 2011;30(3): 253–264.
38. Chiaradonna F, Sacco E, Manzoni R, Giorgio M, Vanoni M, Alberghina L. Ras-dependent carbon metabolism and transformation in mouse fibroblasts. *Oncogene*. 2006;25(39):5391–5404.
39. Sonveaux P, Végran F, Schroeder T, et al. Targeting lactate-fueled respiration selectively kills hypoxic tumor cells in mice. *J Clin Invest*. 2008;118(12):3930–3942.
40. Bini L, Magi B, Marzocchi B, et al. Protein expression profiles in human breast ductal carcinoma and histologically normal tissue. *Electrophoresis*. 1997;18(15):2832–2841.
41. Kabbage M, Chahed K, Hamrita B, et al. Protein alterations in infiltrating ductal carcinomas of the breast as detected by nonequilibrium pH gradient electrophoresis and mass spectrometry. *J Biomed Biotechnol*. 2008;2008:564127.
42. Hennipman A, van Oirschot BA, Smits J, Rijksen G, Staal GE. Glycolytic enzyme activities in breast cancer metastases. *Tumour Biol*. 1988;9(5):241–248.
43. Zhang D, Tai LK, Wong LL, Chiu LL, Sethi SK, Koay ES. Proteomic study reveals that proteins involved in metabolic and detoxification pathways are highly expressed in HER-2/*neu*-positive breast cancer. *Mol Cell Proteomics*. 2005;4(11):1686–1696.
44. Luo W, Semenza GL. Emerging roles of PKM2 in cell metabolism and cancer progression. *Trends Endocrinol Metab*. 2012;23(11):560–566.
45. Xu SG, Yan PJ, Shao ZM. Differential proteomic analysis of a highly metastatic variant of human breast cancer cells using two-dimensional differential gel electrophoresis. *J Cancer Res Clin Oncol*. 2010;136(10):1545–1556.
46. Cheng T, Sudderth J, Yang C, et al. Pyruvate carboxylase is required for glutamine-independent growth of tumor cells. *Proc Natl Acad Sci U S A*. 2011;108(21):8674–8679.

Funding

This investigation was supported by the National Cancer Institute at the National Institutes of Health (RO1 CA142604-03 to SVS). This research project used the animal facility and the tissue and research pathology facility supported in part by a grant from the National Cancer Institute at the National Institutes of Health (P30 CA047904).

Notes

J. A. Arlotti, J. Lee, and E.-R. Hahm were responsible for the treatment of mice, determination of body weights, necropsy, and collection of tissues. Histopathological evaluations were done by E.-R. Hahm, S.-H. Kim, and A. Sehrawat in close consultation with a board-certified pathologist (R. Bhargava). Immunohistochemical analyses were performed by S.-H. Kim, E.-R. Hahm, and J. Lee. S. S. Shiva was responsible for determination of complex III and complex IV activities. Each listed author contributed to preparation of the initial manuscript draft. S. V. Singh was responsible for the overall experimental design and supervision of the experiments, data interpretation, and preparation of the final manuscript.

Affiliations of authors: University of Pittsburgh Cancer Institute, Pittsburgh, PA (JAA, SVS); Department of Pharmacology and Chemical Biology (E-RH, JL, S-HK, AS, SSS, SVS), Vascular Medicine Institute (SSS), and Department of Pathology (RB), University of Pittsburgh School of Medicine, Pittsburgh, PA.